





The rice germin-like protein OsGLP1 participates in acclimation to UV-B radiation

Zhi-Dan He,¹ Mi-Lin Tao ,¹ David W. M. Leung ,² Xiao-Yu Yan,¹ Long Chen,¹ Xin-Xiang Peng ¹ and E.-E. Liu ^{1,*†}

¹ College of Life Sciences, South China Agricultural University, Guangzhou 510642, China
² School of Biological Sciences, University of Canterbury, Christchurch 8140, New Zealand

*Author for communication: eeliu70@scau.edu.cn

†Senior author.

Z.H., M.T., and E.L. designed the research. Z.H., M.T., X.Y., C.L., and E.L. performed the experiments, analyzed the data. D.L., X.P., and E.L. wrote the manuscript. Z.H. and M.T. contributed equally.

The author responsible for distribution of materials integral to the findings presented in this article in accordance with the policy described in the Instructions for Authors (<https://academic.oup.com/plphys/pages/general-instructions>) is: E.-E. Liu (eeliu70@scau.edu.cn).

Abstract

Exposure to ultraviolet B radiation (UV-B) stress can have serious effects on the growth and development of plants. Germin-like proteins (GLPs) may be involved in different abiotic and biotic stress responses in different plants, but little is known about the role of GLPs in UV-B stress response and acclimation in plants. In the present study, knockout of GLP 8–14 (OsGLP1) using the CRISPR/Cas9 system resulted in mutant rice (*Oryza sativa* L.) plants (herein called *glp1*) that exhibited UV-B-dependent formation of lesion mimic in leaves. Moreover, *glp1* grown under solar radiation (including UV-B) showed decreased plant height and increased leaf angle, but we observed no significant differences in phenotypes between wild-type (WT) plants and *glp1* grown under artificial light lacking UV-B. F_v/F_m , Y (II) and the expression of many genes, based on RNA-seq analysis, related to photosynthesis were also only reduced in *glp1*, but not in WT, after transfer from a growth cabinet illuminated with artificial white light lacking UV-B to growth under natural sunlight. The genes-associated with flavonoid metabolism as well as UV resistance locus 8 (*OsUVR8*), phytochrome interacting factor-like 15-like (*OsPIF3*), pyridoxal 5'-phosphate synthase subunit PDX1.2 (*OsPDX1.2*), deoxyribodipyrimidine photolyase (*OsPHR*), and deoxyribodipyrimidine photolyase family protein-like (*OsPHRL*) exhibited lower expression levels, while higher expression levels of mitogen-activated protein kinase 5-like (*OsMPK3*), mitogen-activated protein kinase 13-like (*OsMPK13*), and transcription factor MYB4-like (*OsMYB4*) were observed in *glp1* than in WT after transfer from a growth cabinet illuminated with artificial white light to growth under natural sunlight. Therefore, mutations in *OsGLP1* resulted in rice plants more sensitive to UV-B and reduced expression of some genes for UV-B protection, suggesting that OsGLP1 is involved in acclimation to UV-B radiation.

Introduction

UV-B light (280–315 nm and herein referred to as UV-B) is an intrinsic part of sunlight reaching the earth's surface. Since plants use sunlight for photosynthesis, inevitably they are exposed to potentially harmful levels of UV-B under natural growth conditions. Sensing low levels of UV-B with

receptor UV resistance locus 8 (UVR8) is known to trigger UVR8-mediated signaling in regulating various aspects of metabolism and development to protect plants against UV-B damage (Jenkins, 2009; Tilbrook et al., 2013). This UVR8-mediated signaling process involves two important light signaling components, namely E3 ubiquitin ligase constitutively

photomorphogenic 1 (COP1) and the transcription factor elongated hypocotyl 5 (HY5). The interaction between COP1 and UVR8 activates the expression of many genes mainly associated with prevention of UV-B damage (Nawkar et al., 2013; Tilbrook et al., 2013). As a feedback regulation, repressor of UV-B photomorphogenesis 1 (RUP1) and RUP2 can disrupt the interaction between COP1 and UVR8 leading to the re-dimerization of UVR8 (Heijde and Ulm, 2013). On the other hand, RUP1/RUP2 could also be degraded following interaction between RUP1/RUP2 and COP1, leading to HY5 stability (Ren et al., 2019). Besides, the interaction of UVR8 with WRKY DNA-binding protein 36 (WRYK36) in the presence of UV-B prevents the inhibition of *HY5* transcription by WRYK36. HY5 plays a role in induction of gene expression by UV-B and result in, for example, suppression of embryonic axis elongation (Yang et al., 2018). Furthermore, UVR8 seems to be able to cross talk with other signaling pathways, particularly auxin signaling, in regulating several responses. For instance, in the presence of UV-B, UVR8 inhibited the DNA-binding activities of MYB domain protein 73/77 (MYB73/MYB77) and directly repressed the transcription of their target auxin-responsive genes (Yang et al., 2020). UVR8 can also interact with methanesulfonate-suppressor (BES1) and BES1-interacting Myc-like 1 (BIM1), which are transcription factors involved in brassinosteroid signaling promoting hypocotyl elongation of Arabidopsis (Liang et al., 2018). By repressing the DNA-binding activities of these transcription factors, UVR8 can affect growth and photomorphogenesis. Moreover, *BES1*-RNAi transgenic plants and *bim123* triple mutants were more sensitive to UV-B treatment (Liang et al., 2018). Similarly, *rup1 rup2* and *rup2* mutants were also more sensitive to narrowband UV-B radiation (Gruber et al., 2010), but *uvr8* (Kliebenstein et al., 2002; Favory et al., 2009), *cop1* (Oravec et al., 2006), *hy5* (Ulm et al., 2004; Brown et al., 2005) mutants were hypersensitive to UV-B stress.

High levels of UV-B can directly damage DNA, lipids, proteins, and photosynthesis apparatus, induce reactive oxygen species production, and affect cell integrity and vitality (Jenkins, 2009). For survival, plants need highly efficient UV-B protective mechanisms/tolerance. The response to UV-B stress involves the mitogen-activated protein kinase (MAPK) signaling cascade. UV-B stress can induce accumulation of MAP kinase phosphatase (MKP1) as well as activation of MKP1-interacting proteins MPK3 and MPK6 in Arabidopsis (González Besteiro et al., 2011; González Besteiro and Ulm, 2013). Single Arabidopsis mutants of *mpk3* and *mpk6* are more resistant to UV-B stress, but *mpk1* mutants are hypersensitive to acute UV-B stress, which is related to sustained activities of MPK3 and MPK6 (González Besteiro et al., 2011). This pathway of MKP1-regulated stress-response is independent of the known signaling response mediated by UVR8. The role of UVR8-dependent pathway in UV-B stress is elusive, although studies have shown that the two independent pathways mediated by MKP1 and UVR8 contribute synergistically to UV-B tolerance in plants (González Besteiro et al., 2011).

Substantial knowledge of molecular, cellular, and organismal responses to UV-B has been achieved in past decades from research mainly undertaken with Arabidopsis grown under artificial light. The activities and relative importance of the UVR8-dependent and -independent pathways in plants growing under sunlight are, however, poorly understood. Since high levels of UV-B can also regulate the expression of many genes through UVR8-independent pathways, there may be other types of UV-B photoreceptors in plants (Nawkar et al., 2013; Liang et al., 2019; Tossi et al., 2019). It is, therefore, necessary to explore the functions and regulation of UVR8 in diverse plant species as well as the activities and importance of UV-B response pathways in plants growing under sunlight.

Germin-like proteins (GLPs) are the proteins that share around 30%–70% identity with germin (Bernier and Berna, 2001) and have diverse enzymatic activities, such as superoxide dismutase (SOD; Segarra et al., 2003; Gucciardo et al., 2007), oxalate oxidase (OxO; Sakamoto et al., 2015), pyrophosphatase/phosphodiesterase (AGPPase; Rodríguez-López et al., 2001; Mansilla et al., 2012) and polyphenol oxidase activity (Cheng et al., 2014). Additionally, they can also act as receptors (Swart et al., 1994; Membré et al., 2000; Gucciardo et al., 2007), protease inhibitor (Mansilla et al., 2012), and may be involved in different abiotic and biotic stress responses in different plants (Das et al., 2019). Little is, however, known about the role of GLPs in UV stress response and tolerance in plants. In a proteomic study, the abundance of a GLP in the leaves of peanut plants kept under supplementary UV-B was reported to be increased (Du et al., 2014). It is, however, not clear if a GLP might also play a role in UV radiation response in rice. In this study, new evidence was obtained in support of the participation of OsGLP1 in UV-B stress response of rice plants based on phenotypic, RNA sequencing (RNA-seq), and reverse transcription quantitative (RT-qPCR) analyses of the *glp1* mutants generated using the CRISPR/Cas9 system. A rice GLP 8–14 (OsGLP1, LOC4345763) is encoded by a member of the germin-like gene family, which shares 90% amino acid identity with adenosine diphosphate glucose pyrophosphatase of barley and wheat, and 80% with the auxin-binding protein ABP20 precursor of corn (*Zea mays* L). Besides alterations to plant architecture, lesion mimic only appeared in the leaves of *glp1* mutants grown under lighting regimes that included UV-B (sunlight or artificial light supplemented with UV-B in a growth chamber). Similarly, the leaves of *uvr8-1* mutants exposed to white light supplemented with UV-B for 3 d also showed necrosis (Kliebenstein et al., 2002). The results obtained in the present study support the hypothesis that OsGLP1 was involved in the acclimation of rice to UV-B.

Results

UV-B-dependent formation of lesion mimic and alterations in plant architecture in *glp1* mutants

Using CRISPR/Cas9 technology, *glp1* mutant rice plants were generated in the Dongjin (DJ) background. Sequence alignment and expression analysis showed that *glp1-3*, *glp1-4*, and

glp1-8 mutants with different mutations in the coding sequence (CDS) of *OsGLP1* were loss-of-function mutants (Supplemental Figure S1). The *glp1* mutant plants displayed phenotypes that differed from those of wild-type (WT). Compared to WT, there were some brown spots on the leaf blades of *glp1* grown under natural sunlight (Figure 1A). Clear trypan blue staining areas showing occurrence of cell death were observed in the leaves of *glp1* mutants grown under sunlight (Supplemental Figure S2). The brown spots appeared in the leaves of *glp1* after transfer from a controlled growth chamber (12-h dark at 28°C and 12 h of 600 $\mu\text{mol m}^{-2} \text{s}^{-1}$ artificial light lacking UV-B at 30°C) to growth under sunlight. There were, however, significantly fewer lesions in the newly grown leaves than in old leaves (Supplemental Figure S3) and in the leaves of seedlings grown under natural sunlight after germination than in those transferred to natural sunlight from white light (Figure 2A; Supplemental Figure 3A). When *glp1* was grown outdoors under a piece of glass or in a glasshouse whereby natural sunlight was filtered through, the abundance of the lesions in the leaf blades decreased remarkably compared to those of *glp1* grown under 50–100 $\mu\text{W cm}^{-2}$ UV-B in the glasshouse supplemented with extra UV-B (Supplemental Figure S4). On the other hand, lesions were not observed in the leaves of *glp1* mutant plants grown in a controlled growth chamber (12-h dark, 28°C/12-h light, 30°C) under 600 $\mu\text{mol m}^{-2} \text{s}^{-1}$ artificial light lacking UV-B compared to those of *glp1* kept in a growth room supplemented with 50–80 $\mu\text{W cm}^{-2}$ UV-B (Figure 1B). These results suggest that

UV-B triggered the lesion development in the *glp1* knockout mutants. To explore the possibility that formation of leaf lesions in the *glp1* mutants could be specifically dependent on UV-B or a combination of environmental factors other than UV-B, transgenic plants grown to the 4-leaf stage in a growth chamber without supplementary UV-B were then placed at different conditions as described in Supplemental Figure S4. Interestingly, high light intensity and high temperature could not induce the appearance of lesions in the leaves of the *glp1* (Supplemental Figure S4). Therefore, the formation of lesions in the leaves of *glp1* appears to be dependent on UV-B.

Besides lesion formation, *glp1* grown under natural sunlight also showed decreased plant height and root length as well as increased leaf angle at the 5-leaf stage (Figure 2, A–D). In contrast, there was no apparent difference in the phenotypes between WT and *glp1* grown in a controlled growth chamber illuminated with artificial light lacking UV-B (Figure 2, E–H). Phenotypes including increased leaf angle as well as semi-dwarf plants became more prominent in *glp1* grown under natural sunlight at the maturation stage (Supplemental Figure S5, A–C). There was no significant difference in stem length between WT and *glp1* grown in a glasshouse, although the leaf angle of *glp1* was greater than WT. It is important to note that this increase in leaf angle in *glp1* grown in the glasshouse was less than when grown under natural light (Supplemental Figure S5, D–F). Taken together, these results have revealed a heretofore unrecognized role for *OsGLP1* in UV-B protection and UV-B-triggered responses.

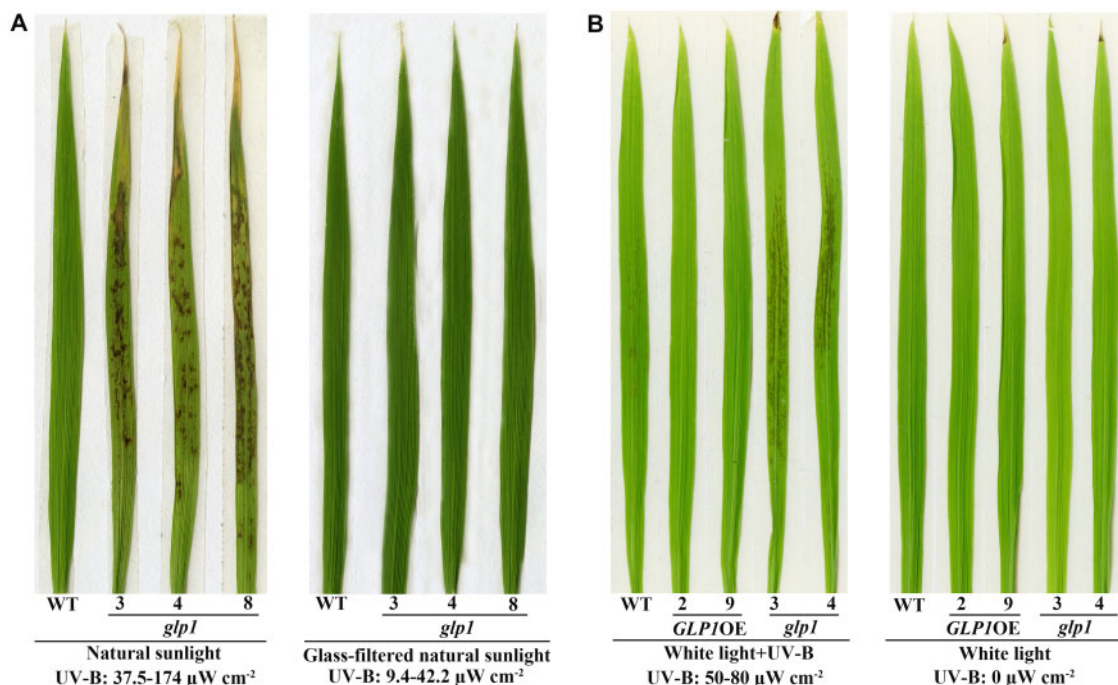


Figure 1 Appearance of the lesion mimic on leaves of rice *glp1* mutants. A, is the second leaves from bottom to top of WT, transgenic plants overexpressing *OsGLP1* (2 and 9) and *glp1* mutants (3, 4, and 8) grown in a growth chamber without UV-B (12 h of 600 $\mu\text{mol m}^{-2} \text{s}^{-1}$ artificial light at 30°C and 12 h of dark at 28°C) to 5-leaf stage and then exposed to natural sunlight and natural sunlight passing through a glass for 1.5 d. B, is the second leaves from bottom to top of 5-leaf stage seedlings grown in a controlled growth chamber with (left) or without (right) 50–80 $\mu\text{W cm}^{-2}$ UV-B for 5 h, and were then grown in the chamber without UV-B for 30 h.

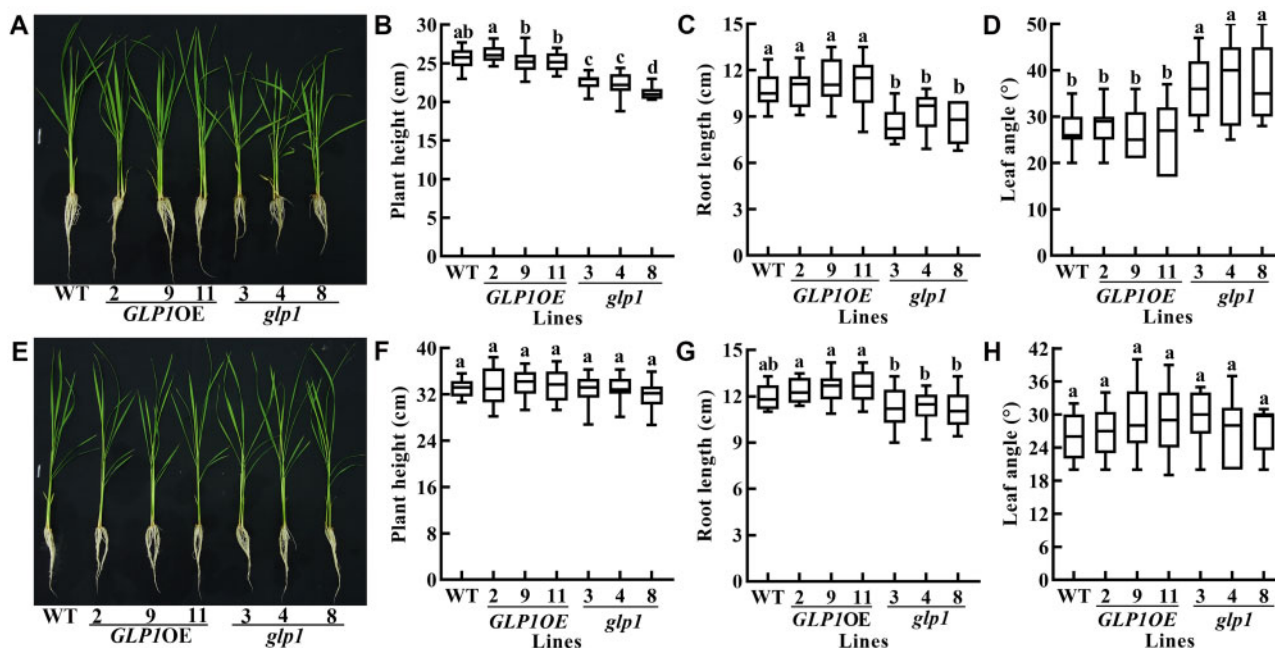


Figure 2 Knockout of *OsGLP1* results in dwarfism and increased leaf inclination in rice plants grown under natural sunlight. In A, B, C, and D, the phenotype, plant height, root length and leaf angle (the second leaf from bottom to top), respectively, of WT, transgenic plants overexpressing *OsGLP1* (2, 9, and 11) and *glp1* mutants (3, 4, and 8) grown under natural sunlight until the 5-leaf stage are shown. In E, F, G, and H, the phenotype, plant height, root length and leaf angle, respectively, of WT, transgenic plants overexpressing *OsGLP1* (2, 9, and 11) and *glp1* mutants (3, 4, and 8) grown in a controlled growth chamber deficient in UV-B (12-h light, $600 \mu\text{mol m}^{-2} \text{s}^{-1}$, 30°C ; 12-h dark, 28°C) until the 5-leaf stage are shown. The boxplots, from top to bottom, denote maximum value, upper quartile, median, lower quartile and minimum value, and whiskers denote maximum value to minimum value of the data. The means \pm SD ($n \geq 16$ plants) of plant height, root length or leaf angle assigned with different letters were significantly different as determined by one-way analysis of variance (ANOVA) with post hoc Bonferroni test ($P < 0.05$).

More damages on photosynthetic efficiency in *glp1* than in WT plants transferred from artificial white light to growth under natural sunlight

The photosynthetic organs of plants are very sensitive to UV-B. The parameters related to photosynthesis were, therefore, measured in WT, *glp1*, and *OsGLP1OE* plants. Compared to WT, the net photosynthesis rate but not the stomatal conductance in *glp1* at the 6-leaf stage was decreased after transfer to growth under natural sunlight for 2 h from a controlled growth chamber deficient in UV-B, but this decrease in net photosynthesis rate in *glp1* did not take place after transfer to a glasshouse (without any supplementation of UV-B) for 2 h (Figure 3, A and B). Moreover, F_v/F_m and $Y(II)$ of *glp1* displayed a significant decrease after transfer to growth under natural sunlight for 8 h. No significant difference in F_v/F_m and $Y(II)$ was observed between WT and *glp1* grown in a growth chamber under artificial light without any supplementation of UV-B (Figure 3, C and D). Taken together, these results suggest that there was more damage to photosystem in the *glp1* under sunlight and are also consistent with the suggestion that *glp1* may play a role in UV-B acclimation.

The abundance and location of *OsGLP1* are unaffected by UV-B irradiation

To explore the role of *OsGLP1* in UV-B signal transduction, regulation of *OsGLP1* by UV-B was investigated. Based on

the Western blotting results (Figure 4, A and B), there was no significant difference in the levels of *OsGLP1* whether WT at the 4-leaf stage or 7-d-old *OsGLP1-GFP* seedlings were exposed to $50\text{--}80 \mu\text{W cm}^{-2}$ of UV-B for 3 or 2 h, respectively. Similarly, the abundance of UVR8 was also unaffected by $3 \mu\text{mol m}^{-2} \text{s}^{-1}$ UV-B, but UV-B could affect its subcellular location (Kaiserli and Jenkins, 2007).

When leaf sheath from 7-d-old seedlings overexpressing *GLP1-GFP* grown under white light lacking UV-B were examined using confocal microscopy, the fluorescence dots were found mainly in the cell margins and a few in the cytosol (Figure 4C), and some were moving during microscopic observation. There was, however, no obvious difference in the localization of the fluorescence when the seedlings overexpressing *GLP1-GFP* placed under white light supplemented with $50\text{--}80 \mu\text{W cm}^{-2}$ UV-B for 2 h during microscopic observation (Figure 4E). Plasmolysis of leaf sheaths using 30% sucrose showed some dots were in the extracellular space (Figure 4D), but fluorescence dots were mainly found in the cytosol of protoplasts isolated from WT transfected with pB121-*GLP1-GFP* (Supplemental Figure S6).

OsGLP1 encodes a protein devoid of detectable SOD activity and OxO activity

The amino acid sequence identity between *OsGLP1* and a GLP of wheat (*TaGLP1*) is 90% (Supplemental Figure S7). Both have previously been reported to have SOD activity

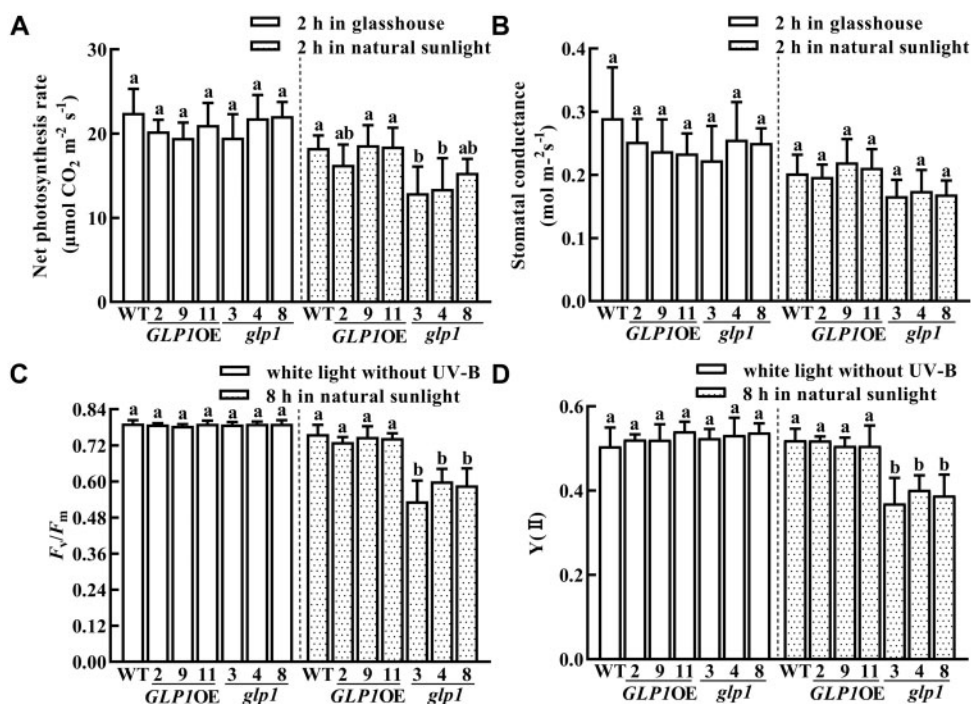


Figure 3 Knockout of *OsGLP1* results in lower photosynthetic efficiency in *glp1* compared to those in WT plants transferred from white light to natural sunlight. Determination of net photosynthesis rate (A), stomatal conductance (B), F_v/F_m (C), and $Y(II)$ (D) in leaves of WT, transgenic plants overexpressing *OsGLP1* (2, 9, and 11) and *glp1* mutants (3, 4, and 8). All the plants were grown to the 6-leaf stage in a growth chamber (conditions of the growth chamber: $600 \mu\text{mol m}^{-2} \text{s}^{-1}$ white light, $0 \mu\text{W cm}^{-2}$ UV-B, 12 h, 30°C ; dark, 12 h, 28°C). They were then exposed to different experimental conditions as specified on the figure: under glasshouse conditions, natural sunlight ($320\text{--}1080 \mu\text{mol m}^{-2} \text{s}^{-1}$, $21.1\text{--}112.9 \mu\text{W cm}^{-2}$ UV-B, $26^\circ\text{C}\text{--}29^\circ\text{C}$) or white light without supplementation of UV-B. From the comparative analysis of the data obtained under a specific experimental condition, the means \pm SD ($n \geq 4$ plants) assigned with different letters were significantly different as determined by one-way ANOVA with the means separation post hoc Student–Newman–Keuls test ($P < 0.05$).

(Segarra et al., 2003; Banerjee and Maiti, 2010). Here, using a test-tube colorimetric enzyme assay and in-gel enzyme activity staining, no difference in SOD activity was found in the crude protein extracts from WT, transgenic plants overexpressing *OsGLP1* and *glp1* mutants placed under natural sunlight for 8 h before SOD assay (Figure 5A; Supplemental Figure S8). In contrast, *OsGLP1* abundance displayed a substantial increase in *GLP1OE* plants and it was knocked out in *glp1* (Supplemental Figure S1). No OxO activity could be detected in leaves of WT, *glp1*, and *GLP1OE* plants using the colorimetric method. Therefore, *OsGLP1* was a protein that lacked detectable activities of SOD and OxO. Moreover, 3, 3'-diaminobenzidine (DAB) staining and nitrotetrazolium blue chloride (NBT) staining showed that *glp1* had slight lower contents of H_2O_2 and $\text{O}_2^{\cdot-}$, respectively, than WT and transgenic rice plants overexpressing *OsGLP1* (Figure 5, C and D).

OsGLP1 mutation causes reduced expression of some genes in UVR8 signaling pathway and increased *MPK3* and *MPK13* transcripts in MAPK signaling cascade

To gain insight into the molecular basis of UV-B-dependent *glp1*-related lesion mimic formation in rice, total RNA was extracted for RNA-seq from leaves of WT and *glp1* at the

4-leaf stage transferred to growth under natural sunlight for 0 h, 4 h, and 8 h from a controlled growth chamber (12-h dark at $28^\circ\text{C}/12$ h artificial light of $600 \mu\text{mol m}^{-2} \text{s}^{-1}$ without UV-B supplementation at 30°C). It was found that 304, 4,538, and 4,215 genes were upregulated at least two-fold, while 31, 3,194, and 4,562 genes were downregulated at least two-fold in *glp1* compared with WT after exposure to 0 h, 4 h, and 8 h under natural sunlight, respectively (Figure 6). The RNA-seq results suggest that transcriptional reprogramming occurred in *glp1* prior to the onset of lesion formation (Figure 6, A and B; Supplemental Figure S9A and Supplemental datasets S1–8). The results of pathway enrichment analyses revealed that the genes mainly involved in photosynthesis, carbon metabolism, flavone, and flavonol biosynthesis were affected in *glp1* (Figure 6C; Supplemental Figure S9B).

Validation using RT-qPCR of the changes in the expression of the following selected genes that seem to be associated with UV-B exposure based on the RNA-seq results was carried out (Figure 7; Supplemental Figure S10): cryptochrome 1a, (*OsCRY1a*), phytochrome A (*OsPhyA*), phytochrome B (*OsPhyB*), *OsUVR8a*, *OsUVR8b*, *OsCOP1*, *OsHYS*, PHYTOCHROME-INTERACTING FACTOR-LIKE 15-like (*OsPIF3*), chalcone synthase 1 (*OsCHS1*), pyridoxal 5'-phosphate synthase subunit PDX1.2 (*OsPDX1.2*), deoxyribodipyrimidine photolyase (*OsPHR*),

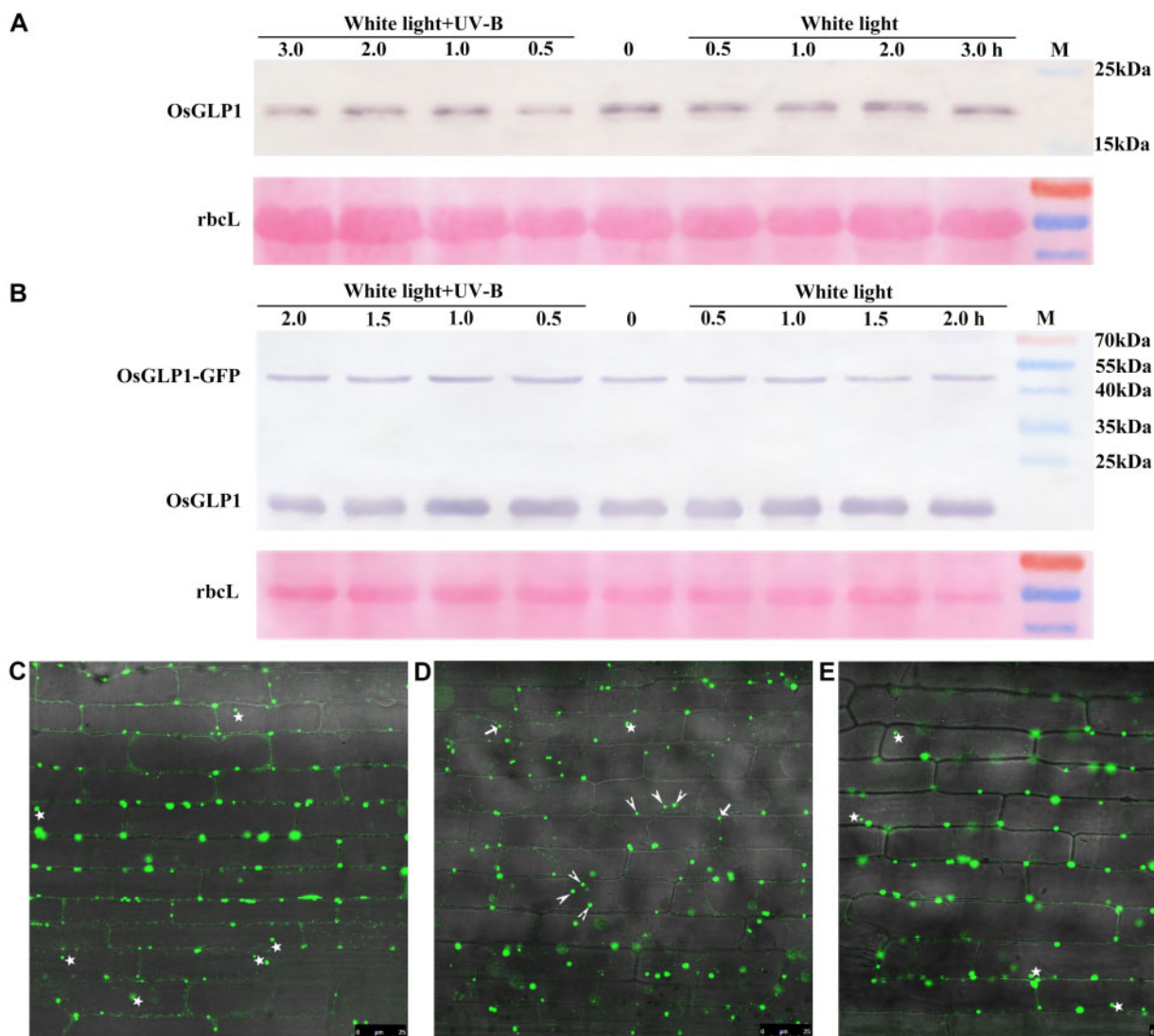


Figure 4 Effect of UV-B on GLP1 and GLP1-GFP protein levels as well as location. Protein gel blot, with OsGLP1-His antisera, of total protein extracts from the leaves of WT (A) grown to 4-leaf stage under $600 \mu\text{mol m}^{-2} \text{s}^{-1}$ white light in a growth chamber deficient in UV-B, and *GLP1-GFP* seedlings grown in the dark on Murashige and Skoog (MS) medium for 7 d (B) before they were exposed to $600 \mu\text{mol m}^{-2} \text{s}^{-1}$ white light supplemented with or without $50\text{--}80 \mu\text{W cm}^{-2}$ UV-B for different times (hours). Confocal images of GFP fluorescence in leaf sheath of transgenic plants expressing GLP1-GFP from the Ubi promoter grown in the dark on MS medium for 7 d before they were exposed to white light and white light supplemented $50\text{--}80 \mu\text{W cm}^{-2}$ UV-B for 2 h (C and E, respectively); confocal images of GFP fluorescence in leaf sheath from *GLP1-GFP* seedlings exposed to white light for 2 h, treated with 30% sucrose about 5 min (D). Bars = 25 μm . Stars denote fluorescence in the cell, short arrows and long arrows denote fluorescence in the plasma membrane and apoplast, respectively.

deoxyribodipyrimidine photolyase family protein-like (*OsPHRL*), *OsMKP1*, MAPK *OsMPK3*, *OsMPK6*, *OsMPK12*, and *OsMPK13* as well as transcription factor MYB4-like (*OsMYB4*). At 0 h (the time before the plants were transferred to natural sunlight), there were no significant differences in the expression of these genes except *HYS*, *MPK3*, *MYB4*, and *PHYA* between WT and *glp1*. Following 8 h of exposure to natural sunlight, however, these genes except *COP1*, *MKP1*, *MKP12*, and *MPK6* were clearly differentially regulated in *glp1*. The vast majority of the RT-qPCR analyses are consistent with the RNA-seq results, and the expression levels of most genes were synergistically regulated by light and genotype (Supplemental Table S1). Moreover, mutating *MPK3* using CRISPR-Cas9 in *glp1-8* plants

abated the formation of lesion (Supplemental Figure S11). These findings further gave credence to the suggestion that OsGLP1 seems to play an intriguing role in UV-B protection by involving the modulation of expression of a range of genes in UVR8-mediated and MAPK signaling cascade pathways.

Expression of *OsGLP1* and genes associated with IAA metabolism modulated in *glp1*

Based on BLAST search of the protein databases, many GLPs in rice can be classified into five phylogenetic subgroups (Supplemental Figure S12) referring to Carrillo et al. (2009). OsGLP1 belongs to the auxin-binding protein subgroup of GLPs, although the only member of this subgroup in peach,

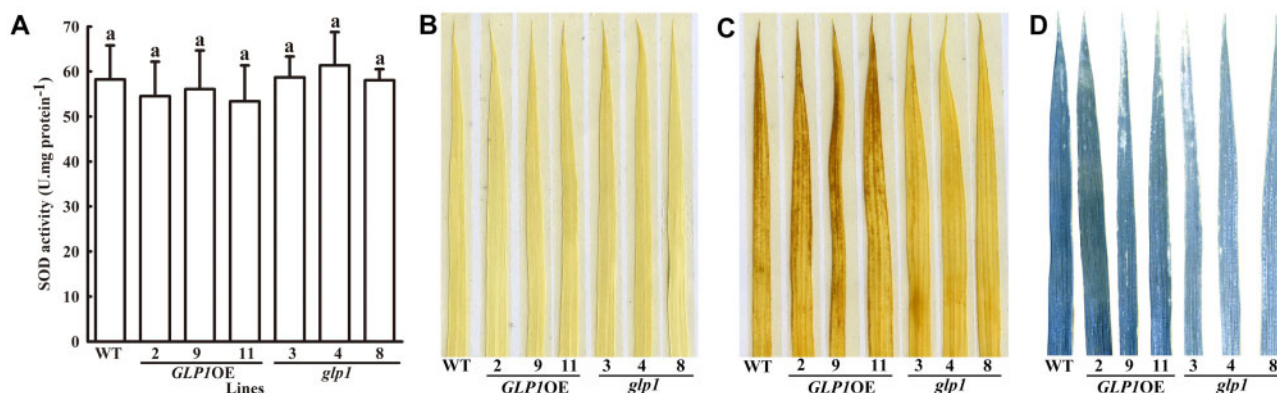


Figure 5 *OsGLP1* encodes a protein devoid of detectable SOD activity. The levels of SOD activity (A), in situ staining for detection of H_2O_2 using DAB (C), $O_2^{\cdot-}$ using NBT (D), and staining control (water only, B) in rice leaves of WT, transgenic plants overexpressing *OsGLP1* (2, 9, and 11) and *glp1* mutants (3, 4, and 8) grown in a growth chamber without UV-B ($600 \mu mol m^{-2} s^{-1}$ white light, 12 h, $30^\circ C$; dark, 12 h, $28^\circ C$) to the 5-leaf stage and then exposed to natural sunlight for 8 h. The means \pm SD ($n = 3$) of SOD activity assigned with the same letter were not significantly different as determined by one-way ANOVA with post-hoc Student–Newman–Keuls test ($P < 0.05$).

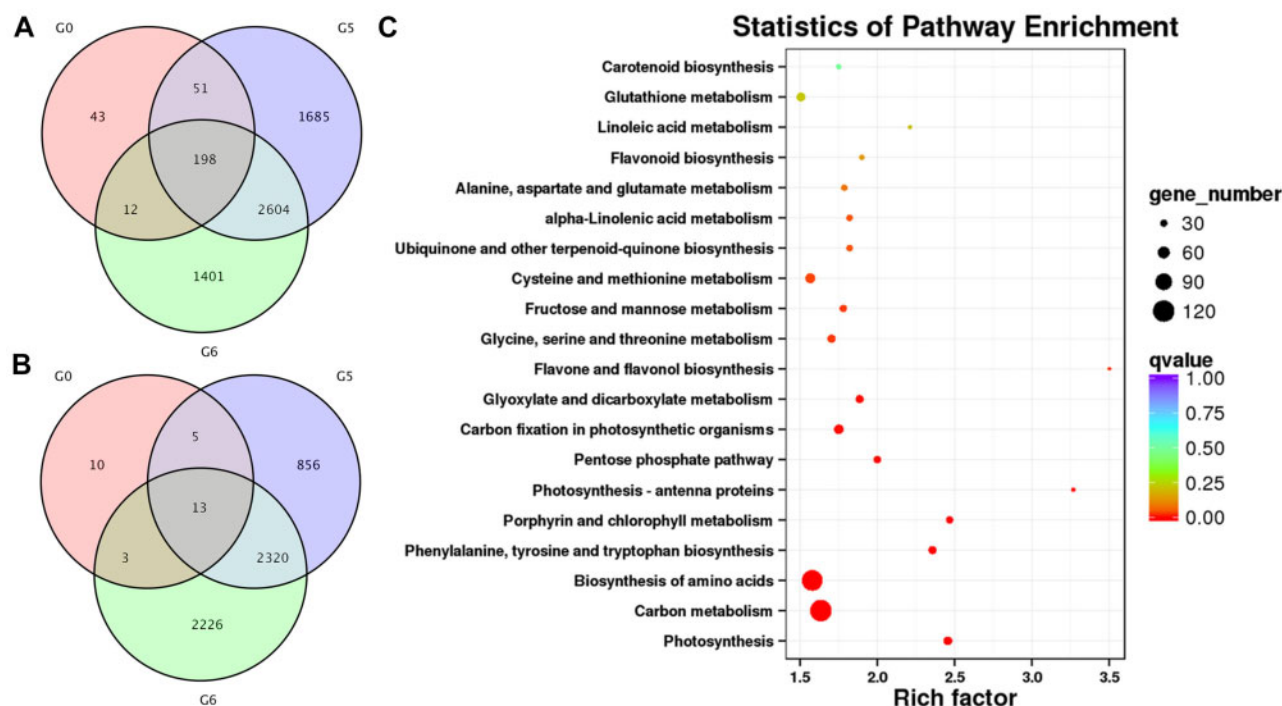


Figure 6 RNA-Seq analyses revealed that many genes are regulated in the leaves of *glp1* mutant transferred from white light to natural sunlight. In A and B, numbers of genes that were upregulated and downregulated in the second leaf from bottom to top of *glp1* seedlings by at least two-fold compared to those in WT are shown, respectively. G0, G5, and G6 denote those in WT and *glp1-4* grown in a growth chamber under $600 \mu mol m^{-2} s^{-1}$ constant white light without UV-B (12-h light, $30^\circ C$; 12-h dark, $28^\circ C$) to the 4-leaf stage and then transferred under natural sunlight for 0 h ($600 \mu mol m^{-2} s^{-1}$, $0 \mu W cm^{-2}$ UV-B, $30^\circ C$), 4 h ($1440 \mu mol m^{-2} s^{-1}$, $174 \mu W cm^{-2}$ UV-B, $37^\circ C$), and 8 h ($810 \mu mol m^{-2} s^{-1}$, $80.2 \mu W cm^{-2}$ UV-B, $35^\circ C$), respectively. Statistics of pathway enrichment analyses of the differentially regulated genes in WT and *glp1-4* grown under natural sunlight for 8 h (C). Scale bar denotes the q value.

ABP19/20, has been shown to bind auxin (Ohmiya et al., 1998). RT-qPCR analysis showed that although *OsGLP1* transcripts were detectable in various tissues, the expression was relatively stronger in the leaf sheath, leaf, and stem of WT (Figure 8A). The expression levels *OsGLP1* increased rapidly in the leaves of WT following the treatment with IAA or NAA. The *OsGLP1* transcript was about three-fold of that in control (treatment with Kimura B complete nutrient solution only) after the treatment

with IAA or NAA for 2 h (Figure 8, B and C). Based on the results of RNA-seq, many genes related to IAA metabolism were changed, including an increase in the transcripts of probable indole-3-acetic acid-amido synthetase GH3.6 (*OsGH3.6*), GH3.8 (*OsGH3.8*), and auxin-responsive protein SAUR71 (*OsSAUR71*), and a reduction in the transcripts of auxin response factor 15-like (*OsARF15*), auxin-responsive protein *OsIAA24*, *OsIAA21*, and *OsIAA13* in *glp1* exposed to natural sunlight for 4 h and 8 h

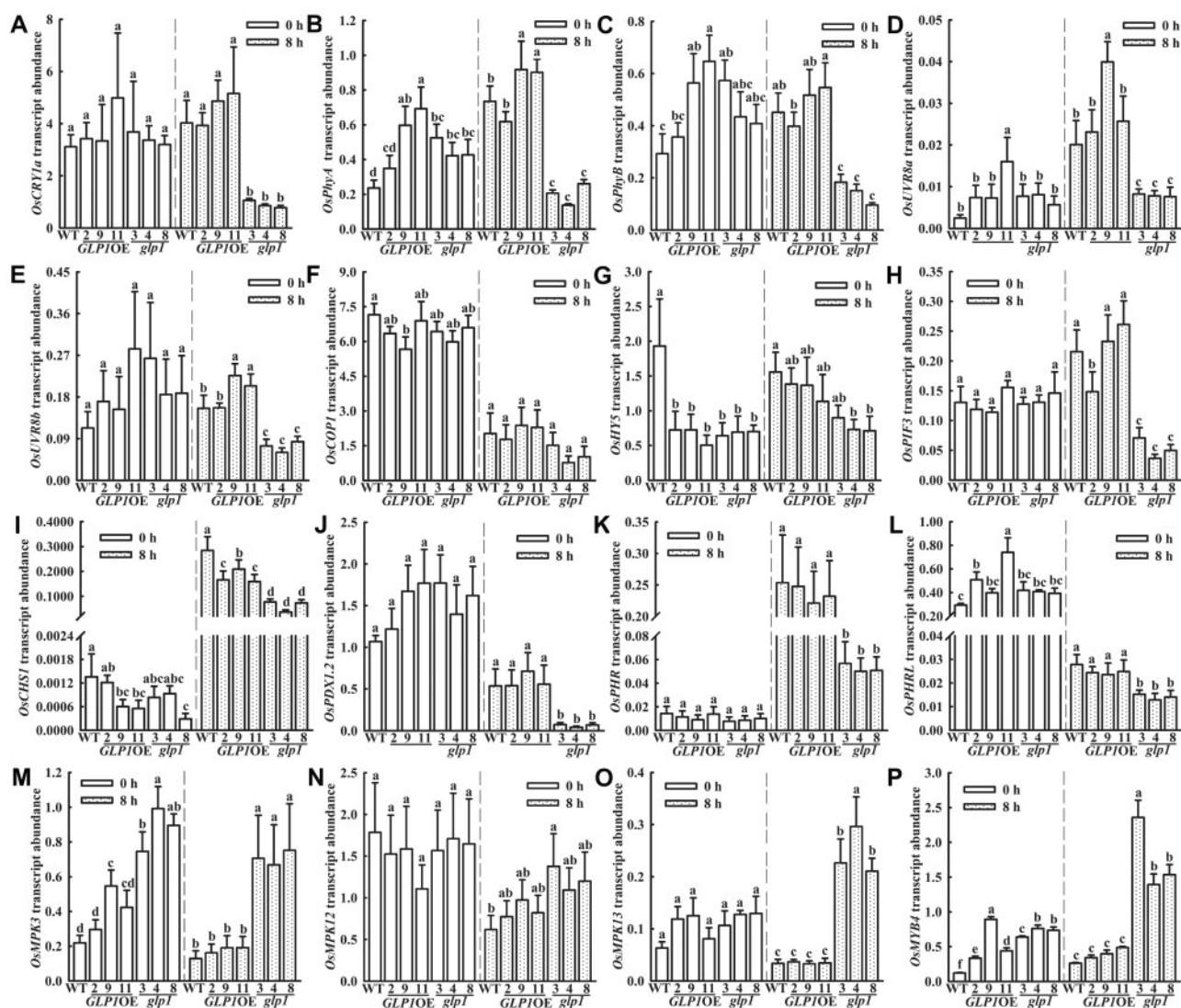


Figure 7 RT-qPCR analysis of the expression of UV-B-associated genes regulated in *gpl1* compared to WT. WT, transgenic plants overexpressing *OsGLP1* (2, 9, and 11) and *gpl1* mutants (3, 4, and 8) were grown in a growth chamber under $600 \mu\text{mol m}^{-2} \text{s}^{-1}$ constant white light (12-h light, 30°C ; 12-h dark, 28°C) to the 4-leaf stage, then transferred to natural sunlight for 0 h ($600 \mu\text{mol m}^{-2} \text{s}^{-1}$, $0 \mu\text{W cm}^{-2}$ UV-B, 30°C) and 8 h ($891.3 \mu\text{mol m}^{-2} \text{s}^{-1}$, $96.4 \mu\text{W cm}^{-2}$ UV-B, 34°C), respectively, and the second leaf from bottom to top of the seedlings were harvested separately. Expression levels of *OsCRY1a* (A), *OsPhyA* (B), *OsPhyB* (C), *OsUVR8a* (D), *OsUVR8b* (E), *OsCOP1* (F), *OsHY5* (G), *OsPIF3* (H), *OsCHS1* (I), *OsPDX1.2* (J), *OsPHR* (K), *OsPHRL* (L), *OsMPK3* (M), *OsMPK12* (N), *OsMPK13* (O), and *OsMYB4* (P) were analyzed and *ACTIN* was used as an internal standard. The mean gene expression levels \pm SD ($n = 3$) in the different plants exposed to natural sunlight at 0 h were compared statistically and those assigned with different letters were significantly different. The same analyses were performed with the plants exposed to natural sunlight for 8 h. All analyses were determined using one-way ANOVA with the means separation post hoc Student–Newman–Keuls test ($P < 0.05$).

(Supplemental dataset S3). Moreover, in an assay of auxin-induced gene expression in plant using *pDR5: GUS* reporter, the *GUS* staining in the leaf cushions of *gpl1* grown under natural sunlight was much lighter than that of WT, but nearly similar to that of WT plants grown under artificial light without supplementation of UV-B in a growth chamber (Supplemental Figure S13).

Discussion

UV-B is a trigger for the formation of leaf lesions and changes in other growth parameters in *gpl1*

The following lines of evidence support the notion that UV-B is a trigger for the formation of lesions in *gpl1*. At the 2-

leaf stage, brown spots began to appear in the leaves of *gpl1* mutants transferred from a growth chamber illuminated with artificial white light deficient in UV-B to growth under natural sunlight. In contrast, there was a notable reduction in the number of lesions in the leaves of *gpl1* grown under natural sunlight filtered through a glasshouse. Although the light intensity and temperature in the glasshouse were comparable to outdoors, the UV-B intensity in the glasshouse was only about 20% of that in natural sunlight. Additionally, when *gpl1* mutants were placed in a glasshouse supplemented with UV-B, a reduction of lesions did not occur. Upon transfer to a growth chamber supplemented with 50-

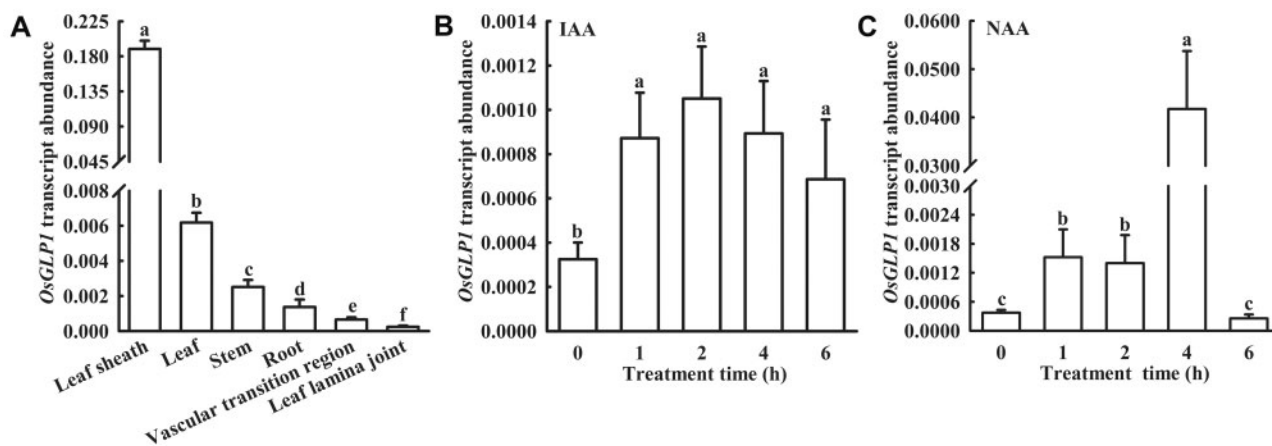


Figure 8 Analysis of *OsGLP1* expression using RT-qPCR. *OsGLP1* expression in various tissues of booting stage rice (A) and in leaves of rice seedlings at the 5-leaf stage treated with 10 $\mu\text{mol L}^{-1}$ IAA (B) and 1 $\mu\text{mol L}^{-1}$ NAA (C) at various time points was analyzed and *ACTIN* was used as an internal standard. The means \pm sd ($n=3$) of gene expression levels assigned with different letters were significantly different as determined by one-way ANOVA with Student–Newman–Keuls test ($P < 0.05$).

80 $\mu\text{W cm}^{-2}$ UV-B, brown spots appeared in the leaves of *glp1*, WT and *GLP1OE* plants exposed to UV-B 3 h, 5 h, and 7 h, respectively. In a prior study involving downregulation of *OsGLP1* using hairpin RNA silencing approach, lesions on the leaves of the transgenic rice plants, and not the untransformed control, were also apparent, but the possibility that these would be lesion mimics was not recognized (Figure 3B in Banerjee and Maiti, 2010). This was probably because the transgenic plants were assumed to be infected by blast fungi and sheath blight as the plants were grown under irrigation in a region known to be disease-prone and the transgenic plants were likely to be more susceptible to diseases compared to the untransformed control (Banerjee and Maiti, 2010). This assumption may be, however, not the sole possible explanation for the lesions on the leaves. Since the plants were grown outdoors, arguably the lesions found on the rice leaves in this prior study could also be induced by UV-B as shown in the present study. Besides, there was no corroborative evidence that the transgenic plants in the study of Banerjee and Maiti (2010) were diseased as they were not inoculated with any sheath blight pathogen or blast fungi.

Ultraviolet light has also been implicated in a prior study of the lesion mimic rice mutant generated from deletion of the heat stress transcription factor *OsSpl7*. When adult *spl7* mutants were grown in summer under natural field conditions (30°C–35°C), there was a high density of lesions on the leaves. If ultraviolet light in solar radiation (presumably UV-B) was filtered out, the number of lesions was drastically reduced (Yamanouchi et al., 2002). Lesions were not observed on the mutant plants grown in a controlled growth chamber (26°C, artificial light), and only few lesions appeared in a high-temperature growth chamber (35°C, artificial light). It seems, therefore, that high temperature and ultraviolet light were both needed to trigger the *spl7* mutants to produce a high density of lesions (Yamanouchi et al., 2002). Other environmental factors including

temperature, light intensity, and sunshine duration have all been previously shown to be associated with the formation of lesions in rice leaves (Wang et al., 2005, 2015; Zhao et al., 2017). For example, brown necrotic lesions appeared in the mature leaves of antisense transgenic rice plants with reduced expression of a rice zinc finger protein (*OsLSD1*) grown at low temperature (21.9°C) and short daylight (11–12 h; Wang et al., 2005). In the present study, however, high light intensity and high temperature could not induce lesion formation in the leaves of *glp1* mutants. UV-B seems, therefore, to be the only requisite trigger for the formation of leaf lesions in *glp1*. Moreover, *Arabidopsis uvr8-1* mutants showed enhanced UV-B sensitivity including exhibition of necrosis in the first true leaves and cotyledons compared to WT when grown for 3 d under constant 0.2 kJ UV-B. Leaf necrosis was progressively more severe during 3 d of recovery under white light deficient in UV-B (Kliebenstein et al., 2002). In the present study, knockout of *OsGLP1* may also make rice plants more sensitive to UV-B as far as induction of necrosis in the leaves and alteration of phenotype are concerned.

Plants exposed to UV-B exhibit a dwarf phenotype as UV-B can greatly inhibit hypocotyl and stem elongation (Jansen, 2002). The reduction in plant height has, therefore, become an important parameter to determine the sensitivity of plants to UV-B radiation. Additionally, UV-B can also affect the growth and development of roots (Ge et al., 2010; Yang et al., 2020). Our results showed that the phenotype of *glp1* was comparable with WT and *OsGLP1OE* seedlings under white light deficient in UV-B (12 h of 600 $\mu\text{mol m}^{-2} \text{s}^{-1}$ artificial light at 30°C and 12 h of dark at 28°C). When grown under natural sunlight, the plant height of *glp1* was, however, about 80% that of WT, and the root length was also shorter than that of WT. The phenotype of *OsGLP1OE* seedlings was not significantly different from WT grown under natural sunlight. In contrast, transgenic rice plants with downregulated expression of *OsGLP1* displayed semi-dwarf

phenotype. Similarly, the cells of the stem were shorter and lower in the length: width ratio in transgenic plants compared to the control reported in a previous study (Banerjee and Maiti, 2010).

After perceiving UV-B signal, UVR8 monomerizes and interacts immediately with COP1, promoting the accumulation of HY5/HYH (Vanhaelewyn et al., 2016). HY5/HYH transcription factor could also control transcription and translation of the auxin transport proteins PIN1 and PIN3 as well as negative regulators of auxin signaling AXR2/IAA7, IAA2, and SLR/IAA14 (Vanhaelewyn et al., 2016). In the present study, RNA-seq analysis showed that the expression of Aux/IAA family members such as *OsIAA2*, *OsIAA3*, *OsIAA10*, *OsIAA17*, *OsIAA24*, etc. was not significantly different from WT before transfer to growth under natural sunlight, but the expression levels of these genes in the leaves of *glp1* were significantly lower than that in WT at 8 h after transfer to growth under natural sunlight. In addition, the GH3 family as a class of genes encoding enzymes that catalyze the conjugation of IAA to amino acids to produce aminoacyl compounds was significantly upregulated in the leaves of *glp1* (Supplemental dataset S3). The transcript of PIFs was also downregulated in *glp1* mutants (Supplemental dataset S6). PIFs are direct regulators of the expression of a number of genes including genes encoding auxin biosynthesis (YUC8/YUC9) and auxin signaling (AUX/IAA; Vanhaelewyn et al., 2016). UV-B can inhibit auxin biosynthesis by triggering degradation of PIF4 and PIF5 and stabilizing DELLA proteins (Hayes et al., 2014), and also inhibit auxin responses through UVR8 (Yang et al., 2020). UV-B can alter the expression of auxin-related genes in plants and cause changes in plant morphological changes (Jansen, 2002). Under natural sunlight conditions, *glp1* showed a typical auxin-deficient phenotype with dwarf and increased angles of flag leaves, as well as decreased auxin content in the leaf lamina. Similarly, *OsLC1* (*OsGH3-1*) function-acquired mutant *lc1-D* also showed dwarf plant phenotype, increased leaf angle, and a decreased free auxin content in the leaf lamina (Zhao et al., 2013). It seems that the alteration in plant height of *glp1* mutants kept under natural sunlight may be due to UV-B-mediated changes in the expression of auxin-related genes in *glp1* mutants.

In addition, the net photosynthetic rate was also reduced in *glp1* mutants after transfer to natural sunlight for 2 h, but not transfer to a glasshouse for 2 h. F_v/F_m and $Y(II)$ in *glp1* also showed a significant decrease when the plants were transferred to natural sunlight for 8 h. These two parameters were not significantly different between WT and *glp1* kept under white light deficient in UV-B. Additionally, the RNA-seq analysis revealed that the expression levels of genes associated with photosynthesis and photorespiration were downregulated in *glp1* after transfer to natural sunlight for 4 h and 8 h (Supplemental dataset S2). Similarly, F_v/F_m and Φ_{PSII} were also decreased in *uvr8* mutants compared to WT exposed to elevated UV-B. It is well known that some photosynthetic components are particularly

susceptible to damage by UV-B, UVR8 is known to promote photosynthetic efficiency at elevated levels of UV-B (Davey et al., 2012). These results in the present study strongly support that knockout of *OsGLP1* resulted in increased sensitivity to UV-B.

OsGLP1 is involved in rice acclimation to UV-B radiation: several genes with UV-B protective roles show altered expression in the *glp1* mutant

Currently, UVR8 is the only known photoreceptor of UV-B. After perceiving UV-B signal, UVR8 orchestrates the expression of a range of genes, such as *HY5*, flavonoid synthesis genes, *PHR* and *PDX*, with vital functions in protecting plants against UV-B and enables plants to survive in sunlight. Accordingly, UV-B signal transduction in *uvr8-1* has been altered as shown by a lack of UV-induced accumulation of flavonoids as well as *CHS* mRNA and protein which is the committing enzyme for flavonoid biosynthesis (Kliebenstein et al., 2002), therefore, *uvr8-1* and *hy5* mutants are highly sensitive to UV-B stress (Brown et al., 2005). In rice genome, two proteins encoded by LOC4329648 (*OsUVR8a*) and LOC4335903 (*OsUVR8b*) share 74% and 75% sequence identity with the Arabidopsis counterpart (*AtUVR8*). Based on RT-qPCR and RNA-seq analyses, there was no significant difference in the expression of *OsUVR8a* and *OsUVR8b* in the WT and *glp1* before transfer from a growth chamber illuminated with artificial white light to outdoors with sunlight. The expression of these genes was significantly lower in the leaves of *glp1* than in WT after transfer to sunlight for 8 h. Similarly, the level of *CHS1* mRNA in *glp1* was also lower than in WT grown under sunlight. Based on the RNA-seq analysis, the expression of genes related to flavonoid metabolism (*Os10g0317900*, *Os10g0317950*, *Os10g0320100*, *Os10g0320201*, and *Os11g0530600*) in the *glp1* was not different from in WT before transfer to outdoors with sunlight. The expression of these five genes in the leaves of *glp1* was, however, significantly downregulated compared to WT after 4 h and 8 h of transfer to natural sunlight (Supplemental dataset S1). Similarly, there is also a lack of UV-B-regulated expression of *CHS* in *uvr8-2* (Brown et al., 2005; Cloix et al., 2012).

In contrast to the expression of *CHS1*, the expression level of *OsMYB4* was upregulated in *glp1* at 8 h after transfer to growth under natural sunlight. Plants overexpressing *AtMYB4* were more sensitive to UV-B. The mutation of *AtMYB4* resulted in increased levels of sinapate esters in Arabidopsis leaves and UV-B tolerance. *AtMYB4* expression is down-regulated by exposure to UV-B light, suggesting that repression of its expression is an important mechanism for acclimation to UV-B in Arabidopsis (Jin et al., 2000). Moreover, the induction of the *OsPHR* transcript in *glp1* grown under natural sunlight was substantially reduced in comparison with WT. This is consistent with a study of Arabidopsis showing that the induction of *AtPHR* transcript by UV-B was also substantially reduced in *uvr8-2* and *uvr8-6* mutants (Li et al., 2015). *PHR* is the repair enzyme for UV-B-

induced cyclobutane pyrimidine dimers which is a principal cause of UV-B-induced growth inhibition in rice grown with supplementary UV-B (Hidema et al., 2007; Teranishi et al., 2012). An increase in PHR activity can significantly alleviate UVB-caused growth inhibition in rice and is essential for protecting cells from UV-B radiation (Li et al., 2015). In addition, the expression level of *OsPDX1.2* in *glp1* was also downregulated. Pyridoxine biosynthesis1 (PDX1) is a protein involved in the synthesis of pyridoxine (vitamin B6) and plays important functions in oxidative stress, photoprotection, and UV-B response (Chen and Xiong 2005; Ristilä et al., 2011). Accumulation of PDX1 under sunlight is modulated by UVR8 (Morales et al., 2013). PDX1.2, MYB4, and PHR all belong to the downstream signaling components of UVR8. Therefore, *OsGLP1* might be involved in the regulation of some genes in UVR8 signaling.

UV-B stress is mediated by activating MAPK signaling pathway. MKP1, MPK3, and MPK6 may play important roles in UV-B signaling and is necessary for UV-B stress resistance in Arabidopsis (González Besteiro et al., 2011). The present RNA-seq analysis showed that the expression levels of MAPK-related genes (*MPK6*, *MKP1*, and *MPK13*) were similar in *glp1* and WT grown under artificial white light deficient in UV-B. The expression levels of *OsMPK1*, *OsMPK3*, *OsMPK6*, *OsMPK12*, and *OsMPK13* were, however, significantly higher in the leaves of *glp1* than in WT grown under natural sunlight for 4 h, while only the *OsMPK3* and *OsMPK13* expression levels were much higher in *glp1* mutant than in WT at 8 h (Supplemental dataset 1). Based on the RT-qPCR analysis, the expression levels of *OsMPK3* and *OsMPK13* were significantly higher in the leaves of *glp1* than in WT grown under natural sunlight for 8 h. The expression level of *OsMPK6* was similar in *glp1* and WT. *OsMPK6* shares 46% identity with *AtMPK4* and has been shown to play a critical role during early embryogenesis because T-DNA insertion mutant of *OsMPK6* is an embryo-lethal mutant (Yi et al., 2016). *OsMPK6* might not be involved in UV-B stress response. Additionally, mutation of *MPK3* in *glp1* mutants could make its lesion lessened in response to solar irradiation (Supplemental Figure S11). *mkp1* seedlings irradiated with broadband UV-B for 3.5 h displayed bleaching and a characteristic dark pigmentation. *MKP1* can provide protection against UV-B-induced cell death by inhibiting UV-induced *MPK3* and *MPK6* activities (González Besteiro et al., 2011), suggesting that the lesion formation in the leaves of *glp1* might be related to MAPK signaling cascade.

In a previous study, TaGLPI, which shares 90% identity with *OsGLP1* is a protease inhibitor with SOD and AGPP activity (Segarra et al., 2003; Mansilla et al., 2012). The results in the present study, however, suggest that *OsGLP1* is devoid of SOD activity, AGPP activity, and protease inhibitor activity based on the in-gel activity assays described by Mansilla et al. (2012). Phylogenetic analysis of 52 GLPs in plants showed that *OsGLP1* belongs to the auxin-binding protein subgroup (Supplemental Figure S12) and has a conserved auxin-binding region Box A (Carrillo et al., 2009).

However, only ABP19/20 in this subgroup has been shown to bind auxin (Ohmiya et al., 1998). Arabidopsis GLP4 could also bind IAA and 2, 4-D as well as its transcript could be stimulated by 10 $\mu\text{mol L}^{-1}$ IAA (Yin et al., 2009). Like *AtGLP4*, the expression of *OsGLP1* could also be induced by IAA and NAA under artificial white light, although it only shares 43% identity with *OsGLP1*. In contrast to *AtGLP4*, another GLP in Arabidopsis, *PDGLP1*, and shares 41% identity with *OsGLP1* localized in the plasmodesmata and was not induced by exogenous IAA treatment. *PDGLP1* could, however, interact with a non-cell-autonomous protein, *NCAPP1*, as well as actin, α β -1, 3-glucanase, phosphate responsive 1, and a putative ABC transporter. In addition, *PDGLP1* could also interact with *PDGLP2* which is found in plasmodesmata-enriched cell wall protein fraction and a regulatory component of root growth and development (Ham et al., 2012). GLPs *AtGER1* and *AtGER3* sharing 62% and 59% identities with *OsGLP1* are also associated with extracellular matrix, but part of *AtGER1* was found in soluble fraction, Membré et al. (2000) proposed that *AtGER1*, *ATGER2*, and *AtGER3* could be a class of receptors involved in physiological, developmental processes and stress response. Moreover, a GLP from pea displayed receptor activity for rhicadhesin (Swart et al., 1994). Similarly, plasmolysis of leaf sheaths of *GLP1-GFP* overexpressing plants showed that fluorescence was found both intracellularly and extracellularly in a dot-like manner. In addition, most GLPs reported up to now are somehow associated with the extracellular matrix, more than half of the GLPs contain a Arg-Gly-Asp/Lys-Gly-Asp (RGD/KGD) tripeptide, which is also present in animal RGD-containing proteins such as fibronectin and vitronectin. In animals, these are adhesion proteins that participate in the exchange of information between the outside and the inside of the cells (Bernier and Berna, 2001). Like the above-mentioned GLPs, *OsGLP1* is also associated with extracellular matrix and contains the auxin-binding region Box A, suggesting that some of the molecular mechanisms whereby *OsGLP1* may be involved in UV-B response in rice.

In conclusion, new insights about UV-B signal transduction in rice acclimating to UV-B have been obtained. The results presented here suggest that *OsGLP1* plays a role in upregulation of UVR8 pathway and repression of the MAPK pathway in response to UV-B. The precise mechanism underpinning these two UV-B response pathways is still elusive and warrants future investigations.

Materials and methods

Plant materials and growth conditions

Rice (*Oryza sativa* L.) cv DJ was used for generating *OsGLP1* knockout mutants and *OsGLP1* overexpressing transgenic rice plants. Germinated seeds were grown in Kimura B complete nutrient solution (Yoshida et al., 1976) under different experimental conditions as described in the legend of each figure. A plant growth chamber (Percival E-41HO) was fitted with fluorescent lamps to supply artificial light. For supplementary UV-B in some experiments, a UV-B lamp (G15T8E

UV-B, with a radiation spectrum of 290–310 nm and a peak at 306 nm, purchased from Sankyo Denki, Kanagawa, Japan) was used. UV intensity was measured using a 742 UV light meter (manufactured by Beijing Normal University, Beijing, China).

Construction of *OsGLP1* mutants and *OsGLP1*-overexpression transgenic plants

OsGLP1 mutants were constructed using the CRISPR/Cas9 system. First, the vector containing a CRISPR cassette comprising a functional Cas9 under an Ubi promoter and two gRNAs with targets at different locations of *OsGLP1* was constructed according to Ma et al. (2015). The vector was then introduced into *Agrobacterium tumefaciens* strain EHA105 for transformation of DJ rice calli using the procedure as described in Hiei et al. (1994). The mutation of *OsGLP1* in transgenic plants regenerated from the transformed rice calli was genotyped by PCR amplification of the target region in DNA extracted from their leaves. The primer sequences used for vector construction and amplification of the target region are listed in Supplemental Table S2. For *OsGLP1OE* vector construction, the full-length *OsGLP1* coding sequence was amplified using PCR with the primers *GLP1-O-L* and *GLP1-O-R* (Supplemental Table S2) and inserted into the pOx vector (provided by professor Yao-Guang Liu, College of Life Sciences, South China Agricultural University, China) containing an Ubi promoter. The *OsGLP1OE* vector construct was introduced into *A. tumefaciens* strain EHA105 for transformation of DJ rice calli according to Hiei et al. (1994). For *OsGLP1-GFP* construct, the full-length *OsGLP1* coding sequence was inserted into pBI121-GFP for rice protoplast transformation, and *OsGLP1-GFP* coding sequence was inserted into pOx for constructing transgenic rice plants overexpressing *OsGLP1-GFP*. Fluorescence signals were observed using WLL laser and HyD detectors of Leica TCS SP8 STED 3X. The excitation/emission filters utilized for fluorescence detection were 488/501–549 nm for GFP, and the gains were 61%. The construct pBI121-*GLP1-GFP* was then introduced into rice protoplasts and the transfected rice protoplasts were sampled for GFP fluorescence observation using argon laser and PMT detectors of Zeiss LSM 7 DUO (Zhang et al., 2011). The excitation/emission filters utilized for fluorescence detection were 488/493–546 nm for GFP, and 488/658–735 nm for chlorophyll autofluorescence, and the gains were 700 for GFP, 790 for *GLP1-GFP*, and chlorophyll autofluorescence.

Total RNA extraction and RT-qPCR analysis

Total RNAs were extracted from various tissues of WT plants or *OsGLP1* transgenic plants with Trizol and reverse-transcribed following the manufacturer's instructions (Vazyme Biotech). RT-qPCR analyses were carried out using a PTC200 (BIO-RAD) PCR machine and a SYBR green probe (Bimake, China). The details of the primers used are given in Supplemental Table S3. *ACTIN* was used as an internal standard and was amplified with *qACTIN* primers.

Determination of photosynthetic parameters and chlorophyll fluorescence

WT, *GLP1OE* plants and *glp1* mutants were grown to the 6-leaf stage in a growth chamber (600 $\mu\text{mol m}^{-2} \text{s}^{-1}$ white light, 0 $\mu\text{W cm}^{-2}$ UV-B, 12 h, 30°C; dark, 12 h, 28°C), and the plants were then placed under natural sunlight or glass-house conditions for 2 h. The net photosynthetic rate (Pn) and stomatal conductance of the third leaf from top to bottom on each plant were determined using a Li-Cor Li-6800 portable photosynthetic apparatus (LI-COR, USA). The air velocity in the system was set to 500 $\mu\text{mol s}^{-1}$ and a built-in light source was used with the light intensity set to 800 $\mu\text{mol m}^{-2} \text{s}^{-1}$. The maximum photochemical efficiency of photosystem II (F_v/F_m) and Y (II) were determined using a DUAL-PAM700 chlorophyll fluorometer after plants were placed under natural sunlight for 8 h or white light without supplementation of UV-B light in a growth room.

SOD activity analysis and immunoblot analysis

WT, *GLP1OE* plants, and *glp1* mutants were grown in Kimura B complete nutrient solution to the 5-leaf stage in a growth chamber (600 $\mu\text{mol m}^{-2} \text{s}^{-1}$ white light, 0 $\mu\text{W cm}^{-2}$ UV-B, 12 h, 30°C; dark, 12 h, 28°C), before they were transferred to natural sunlight for 8 h. Proteins for SOD assay were extracted using 50 mmol L^{-1} PBS buffer (pH 7.8) from leaves of individual transgenic lines and WT. The assay mixture contained 0.3 $\mu\text{mol L}^{-1}$ riboflavin, 13 mmol L^{-1} methionine, 63 $\mu\text{mol L}^{-1}$ nitrotetrazolium blue chloride (NBT) and the enzyme extract in a total volume of 3 mL. The reaction mixture was incubated under 60 $\mu\text{mol m}^{-2} \text{s}^{-1}$ light for 14 min at 25°C before the absorbance was measured at 560 nm. One unit (U) of SOD activity was defined as the enzyme activity that brought about 50% inhibition of photo-oxidative reduction of NBT, and specific SOD activity was expressed as U/mg protein. In-gel detection of SOD activity was performed according to Gucciardo et al. (2007). The proteins from leaves were separated in 7.5% (m/v) native polyacrylamide gel, and then the gel was immersed in 20 mL of 50 mmol L^{-1} PBS buffer (pH 7.8) containing 0.25 mg riboflavin, 4 mg NBT and 50 μL TEMED for about 30 min under light (100 $\mu\text{mol m}^{-2} \text{s}^{-1}$) until visible bands of enzyme activity could be observed. For immunoblotting analysis, proteins were separated by electrophoresis in 13% sodium dodecylsulfate polyacrylamide gel and then electrophoretically transferred to nitrocellulose paper. The *OsGLP1* proteins were detected using *Escherichia coli*-expressed *OsGLP1*-His antiserum as the primary antibodies (prepared in our laboratory), and the alkaline phosphatase-conjugated goat anti-rabbit immunoglobulin (Sigma, St Louis, USA) as the secondary antibodies. For visualization of the *OsGLP1*, the nitrocellulose paper was immersed in 100 mmol L^{-1} Tris-HCl buffer (pH 9.5) containing 100 mmol L^{-1} NaCl, 5 mmol L^{-1} $\text{MgCl}_2 \cdot 6\text{H}_2\text{O}$, 0.2 mmol L^{-1} NBT, and 0.15 mmol L^{-1} 5-bromo-4-chloro-3-indolyl phosphate-toluidine salt.

In situ detection of hydrogen peroxide and superoxide

Hydrogen peroxide (H₂O₂) accumulation was detected using 3, 3'-diaminobenzidine (DAB) staining according to Thordal-Christensen et al. (1997), and superoxide anion (O₂^{•-}) was detected using NBT staining according to May et al. (1996). Leaf blades of rice seedlings at the 5-leaf stage were cut and immersed in 0.5 mg L⁻¹ DAB solution (pH 3.8) and 10 mmol L⁻¹ PBS buffer (pH 7.8) containing 0.5% NBT, respectively, under white light (100 μmol m⁻² s⁻¹) until staining could be observed. Chlorophyll was then removed from the leaf blades by immersing them in industrial-grade alcohol while kept in a boiling water bath.

RNA-seq

The WT and *glp1* mutants were grown to the 4-leaf stage in a growth chamber (600 μmol m⁻² s⁻¹ white light, 12 h, 0 μW cm⁻² UV-B, 30°C; dark, 12 h, 28°C), and then transferred into natural sunlight. The RNA used for RNA-seq analysis was extracted using Trizol from the leaves of WT and *glp1* mutants placed under natural sunlight for 0 h (8:00, 600 μmol m⁻² s⁻¹, 0 μW cm⁻² UV-B, 30°C), 4 h (1440 μmol m⁻² s⁻¹, 174 μW cm⁻² UV-B, 37°C), and 8 h (810 μmol m⁻² s⁻¹, 80.2 μW cm⁻² UV-B, 35°C). RNA-seq libraries were constructed using the New England Biolab Next Ultra RNA Library Prep Kit for Illumina following manufacturer's instructions. RNA-Seq libraries were sequenced on an Illumina HiSeq xTen sequencer to generate 150 bp paired-end reads. The resulting clean reads were mapped to *O. sativa* reference genome (IRGSP_1.0) using TopHat2 with default parameters. Differential expression analysis of *glp1* and WT was performed using the DEseq and the differentially expressed genes were identified using fold change ≥2 and FDR <0.01 as significance cutoffs.

Statistical analysis

Except RNA-seq and the construction of transgenic plants, all experiments were performed two times, and the data were statistically analyzed using MS Excel for Windows. The values in the figures are means ± SD, and significant differences among various treatments were analyzed using the Spss 22 analytical software.

Accession numbers

Sequence information of major genes/proteins mentioned in this article can be found in the National Center for Biotechnology Information by the accession numbers in Supplemental dataset 9.

Supplemental data

The following materials are available in the online version of this article.

Supplemental Figure S1. Molecular evaluation of *glp1* mutants generated by CRISPR-Cas9 system.

Supplemental Figure S2. Measurement of cell death in the leaves of *glp1* mutants.

Supplemental Figure S3. Appearance of the lesion mimic on leaves of the *glp1* mutants at different development stages.

Supplemental Figure S4. The effect of growth conditions on the lesion mimic on leaves of *glp1* mutants.

Supplemental Figure S5. Characterization of rice *glp1* mutants grown under natural condition and in glasshouse.

Supplemental Figure S6. Subcellular location of OsGLP1 in rice protoplast.

Supplemental Figure S7. Alignment of amino acid sequences of OsGLP1 with its homologues.

Supplemental Figure S8. Profiles of SOD isoforms in rice leaves.

Supplemental Figure S9. RNA-Seq analyses.

Supplemental Figure S10. The effect of mutation in OsGLP1 on the transcript levels of MKP1 and MPK6.

Supplemental Figure S11. Appearance of the lesion mimic on leaves of *glp1*, *mpk3*, and *glp1 mpk3* mutants.

Supplemental Figure S12. Phylogenetic analysis of OsGLP1 homologs in rice.

Supplemental Figure S13. Assay of IAA content using pDR5: GUS staining.

Supplemental Table S1. Results of RT-qPCR data analyzed using 2-way analysis of variance.

Supplemental Table S2. Primer sequences used for vector construction and amplification of the target region.

Supplemental Table S3. Primer sequences used for RT-qPCR.

Supplemental datasets S1-9. List of genes regulated in *glp1* compared to WT.

Acknowledgments

We thank Yaoguang Liu (South China Agricultural University) for kindly providing pOX and CRISPR/Cas9 system vectors, Huili Liu and Hai Zhou (South China Agricultural University) for helpful discussions, Qinlong Zhu and Hao Wang (South China Agricultural University) for technical assistance, Menglong Zhuang and Xiaojing Zhang (South China Agricultural University) for GFP fluorescence observation.

Funding

This study was funded by Natural Science Foundation of Guangdong (2020A1515010192) and National Natural Science Foundation of China (31071345).

Conflict of interest statement. No conflict of interest is declared.

References

- Banerjee J, Maiti MK** (2010) Functional role of rice germin-like protein1 in regulation of plant height and disease resistance. *Biochem Biophys Res Commun* **394**: 178–183
- Bernier F, Berna A** (2001) Germins and germin-like proteins: Plant do-all proteins. But what do they do exactly? *Plant Physiol Biochem* **39**: 39545–39554
- Brown BA, Cloix C, Jiang GH, Kaiserli E, Herzyk P, Kliebenstein DJ, Jenkins GI** (2005) A UV-B-specific signaling component

- orchestrates plant UV protection. *Proc Natl Acad Sci USA* **102**: 18225–18230
- Davey MP, Susanti NI, Wargent JJ, Findlay JE, Quick WP, Paul ND, Jenkins GI** (2012) The UV-B photoreceptor UVR8 promotes photosynthetic efficiency in *Arabidopsis thaliana* exposed to elevated levels of UV-B. *Photosynth Res* **114**: 121–131
- Carrillo MGC, Goodwin PH, Leach JE, Leung H, Cruz CMV** (2009) Phylogenomic relationships of rice oxalate oxidases to the cupin superfamily and their association with disease resistance QTL. *Rice* **2**: 67–79
- Chen H, Xiong L** (2005) Pyridoxine is required for post-embryonic root development and tolerance to osmotic and oxidative stresses. *Plant J* **44**: 396–408
- Cheng X, Huang X, Liu S, Tang M, Hu W, Pan S** (2014) Characterization of germin-like protein with polyphenol oxidase activity from *Satsuma mandarina*. *Biochem Biophys Res Commun* **449**: 313–318
- Cloix C, Kaiserli E, Heilmann M, Baxter KJ, Brown BA, O'Hara A, Smith BO, Christie JM, Jenkins GI** (2012) C-terminal region of the UV-B photoreceptor UVR8 initiates signaling through interaction with the COP1 protein. *Proc Natl Acad Sci USA* **109**: 16366–16370
- Das A, Pramanik K, Sharma R, Gantait S, Banerjee J** (2019) In-silico study of biotic and abiotic stress related transcription factor binding sites in the promoter regions of rice germin-like protein genes. *PLoS One* **14**: e0211887
- Du ZK, Li JM, Zhong ZC, Dong M** (2014) A proteomic analysis of *Arachis hypogaea* leaf in responses to enhanced ultraviolet-B radiation. *Acta Ecol Sin* **34**: 2589–2598
- Favory JJ, Stec A, Gruber H, Rizzini L, Oravecz A, Funk M, Albert A, Cloix C, Jenkins GI, Oakeley EJ, et al.** (2009) Interaction of COP1 and UVR8 regulates UV-B-induced photomorphogenesis and stress acclimation in *Arabidopsis*. *EMBO J* **34**: 591–601
- Ge L, Peer W, Robert S, Swarup R, Ye S, Prigge M, Cohen JD, Friml J, Murphy A, Tang D, et al.** (2010) *Arabidopsis* ROOT UVB SENSITIVE2/WEAK AUXIN RESPONSE1 is required for polar auxin transport. *Plant Cell* **22**: 1749–1761
- González Besteiro MA, Bartels S, Albert A, Ulm R** (2011) *Arabidopsis* MAP kinase phosphatase 1 and its target MAP kinases 3 and 6 antagonistically determine UV-B stress tolerance, independent of the UVR8 photoreceptor pathway. *Plant J* **68**: 727–737
- González Besteiro MA, Ulm R** (2013) Phosphorylation and stabilization of *Arabidopsis* MAP kinase phosphatase 1 in response to UV-B stress. *J Biol Chem* **288**: 480–486
- Gruber H, Heijde M, Heller W, Albert A, Seidlitz HK, Ulm R** (2010) Negative feedback regulation of UV-B-induced photomorphogenesis and stress acclimation in *Arabidopsis*. *Proc Natl Acad Sci USA* **107**: 20132–20137
- Gucciardo S, Wisniewski JP, Brewin NJ, Bornemann S** (2007) A germin-like protein with superoxide dismutase activity in pea nodules with high protein sequence identity to a putative rhicadhesin receptor. *J Exp Bot* **58**: 1161–1171
- Ham B, Li G, Kang B, Zeng F, Lucasa WJ** (2012) Overexpression of *Arabidopsis* plasmodesmata germin-like proteins disrupts root growth and development. *Plant Cell* **24**: 3630–3648
- Hayes S, Velanis CN, Jenkins GI, Franklin KA** (2014) UV-B detected by the UVR8 photoreceptor antagonizes auxin signaling and plant shade avoidance. *Proc Natl Acad Sci USA* **111**: 11894–11899
- Heijde M, Ulm R** (2013) Reversion of the *Arabidopsis* UV-B photoreceptor UVR8 to the homodimeric ground state. *Proc Natl Acad Sci USA* **110**: 1113–1118
- Hidema J, Taguchi T, Ono T, Teranishi M, Yamamoto K, Kumagai T** (2007) Increase in CPD photolyase activity functions effectively to prevent growth inhibition caused by UVB radiation. *Plant J* **1**: 70–79
- Hiei Y, Ohta S, Komari T, Kumashiro T** (1994) Efficient transformation of rice (*Oryza sativa* L.) mediated by *Agrobacterium* and sequence analysis of the boundaries of the T-DNA. *Plant J* **6**: 271–282
- Jansen MAK** (2002) Ultraviolet-B radiation effects on plants: induction of morphogenic responses. *Physiol Plant* **116**: 423–429
- Jenkins GI** (2009) Signal transduction in responses to UV-B radiation. *Annu Rev Plant Biol* **60**: 407–431
- Jin H, Cominelli E, Bailey P, Parr A, Mehrstens F, Jones J, Tonelli C, Weisshaar B, Martin C** (2000) Transcriptional repression by AtMYB4 controls production of UV-protecting sunscreens in *Arabidopsis*. *EMBO J* **19**: 6150–6161
- Kaiserli E, Jenkins GI** (2007) UV-B promotes rapid nuclear translocation of the *Arabidopsis* UV-B specific signaling component UVR8 and activates its function in the nucleus. *Plant Cell* **19**: 2662–2673
- Kliebenstein DJ, Lim JE, Landry LG, Last RL** (2002) *Arabidopsis* UVR8 regulates ultraviolet-B signal transduction and tolerance and contains sequence similarity to human regulator of chromatin condensation 1. *Plant Physiol* **30**: 234–243
- Li N, Teranishi M, Yamaguchi H, Matsushita T, Watahiki MK, Tsuge T, Li S, Hidema J** (2015) UV-B-induced CPD photolyase gene expression is regulated by UVR8-dependent and -independent pathways in *Arabidopsis*. *Plant Cell Physiol* **56**: 2014–2023
- Liang T, Mei S, Shi C, Yang Y, Peng Y, Ma L, Wang F, Li X, Huang X, Yin Y, et al.** (2018) UVR8 interacts with BES1 and BIM1 to regulate transcription and photomorphogenesis in *Arabidopsis*. *Dev Cell* **44**: 1–12
- Liang T, Yang Y, Liu H** (2019) Signal transduction mediated by the plant UV-B photoreceptor UVR8. *New Phytol* **3**: 1247–1252
- Ma X, Zhang Q, Zhu Q, Liu W, Chen Y, Qiu R, Wang B, Yang Z, Li H, Lin Y, et al.** (2015) A robust CRISPR/Cas9 system for convenient, high-efficiency multiplex genome editing in monocot and dicot plants. *Mol Plant* **8**: 1274–1284
- Mansilla AY, Segarra CI, Conde RD** (2012) Structural and functional features of a wheat germin-like protein that inhibits trypsin. *Plant Mol Biol Rep* **30**: 624–632
- May MJ, Hammond-Kosack KE, Jones JDG** (1996) Involvement of reactive oxygen species, glutathione metabolism, and lipid peroxidation in the Cf-gene-dependent defense response of tomato cotyledons induced by race-specific elicitors of *Cladosporium fulvum*. *Plant Physiol* **110**: 1367–1379
- Membré N, Bernier F, Staiger D, Berna A** (2000) *Arabidopsis thaliana* germin-like proteins: Common and specific features point to a variety of functions. *Planta* **3**: 345–354
- Morales LO, Brosché M, Vainonen J, Jenkins GI, Wargent JJ, Sipari N, Strid Å, Lindfors AV, Tegelberg R, Aphalo PJ** (2013) Multiple roles for UV RESISTANCE LOCUS8 in regulating gene expression and metabolite accumulation in *Arabidopsis* under solar ultraviolet radiation. *Plant Physiol* **161**: 744–759
- Nawkar GM, Maibam P, Park JH, Sahi VP, Lee SY, Kang CH** (2013) UV-induced cell death in plants. *Int J Mol Sci* **14**: 1608–1628
- Ohmiya A, Tanaka Y, Kadowaki K, Hayashi T** (1998) Cloning of genes encoding auxin-binding proteins (ABP19/20) from peach: significant peptide sequence similarity with germin-like proteins. *Plant Cell Physiol* **39**: 492–499
- Oravecz A, Baumann A, Mate Z, Brzezinska MJ, Oakeley EJ, Adam E, Schafer E, Nagy F, Ulm R** (2006) CONSTITUTIVELY PHOTOMORPHOGENIC1 is required for the UV-B response in *Arabidopsis*. *Plant Cell* **18**: 1975–1990
- Ren H, Han J, Yang P, Mao W, Liu X, Qiu L, Qian C, Liu Y, Chen Z, Ouyang X, et al.** (2019) Two E3 ligases antagonistically regulate the UV-B response in *Arabidopsis*. *Proc Natl Acad Sci USA* **116**: 4722–4731
- Ristilä M, Strid H, Eriksson LA, Strid A, Sävenstrand H** (2011) The role of the pyridoxine (vitamin B6) biosynthesis enzyme PDX1 in ultraviolet-B radiation responses in plants. *Plant Physiol Biochem* **49**: 284–292
- Rodríguez-López M, Baroja-Fernandez E, Zanduetta-Criado A, Moreno-Bruna B, Munoz FJ, Akazawa T, Pozueta-Romero J** (2001) Two isoforms of a nucleotide-sugar

- pyrophosphatase/phosphodiesterase from barley leaves (*Hordeum vulgare* L.) are distinct oligomers of HvGLP1, a germin-like protein. *FEBS Lett* **490**: 44–48
- Sakamoto A, Nishimura T, Miyaki YI, Watanabe S, Takagi H, Izumi S, Shimada H** (2015) In vitro and in vivo evidence for oxalate oxidase activity of a germin-like protein from azalea. *Biochem Biophys Res Commun* **458**: 536–542
- Segarra CI, Casalagué CA, Pinedo ML, Ronchi VP, Conde RD** (2003) A germin-like protein of wheat leaf apoplast inhibits serine proteases. *J Exp Bot* **54**: 1335–1341
- Swart S, Logman TJ, Smit G, Lugtenberg BJ, Kijne JW** (1994) Purification and partial characterization of a glycoprotein from pea (*Pisum sativum*) with receptor activity for rhicadhesin, an attachment protein of Rhizobiaceae. *Plant Mol Biol* **24**: 171–183
- Teranishi M, Taguchi T, Ono T, Hidema J** (2012) Augmentation of CPD photolyase activity in japonica and indica rice increases their UVB resistance but still leaves the difference in their sensitivities. *Photochem Photobiol Sci* **11**: 812–820
- Thordal-Christensen H, Zhang Z, Wei Y, Collinge DB** (1997) Subcellular localization of H₂O₂ in plants: H₂O₂ accumulation in papillae and hypersensitive response during the barley powdery mildew interaction. *Plant J* **11**: 1187–1194
- Tilbrook K, Arongaus AB, Binkert M, Heijde M, Yin R, Ulm R** (2013) The UVR8 UV-B photoreceptor: perception, signaling and response. *Arabidopsis Book* **11**: e0164
- Tossi VE, Regalado JJ, Iannicelli J, Laino LE, Burrieza HP, Escandón AS, Pitta-Álvarez SI** (2019) Beyond Arabidopsis: differential UV-B response mediated by UVR8 in diverse species. *Front Plant Sci* **10**: 780
- Ulm R, Baumann A, Oravecz A, Mate Z, Adam E, Oakeley EJ, Schafer E, Nagy F** (2004) Genome-wide analysis of gene expression reveals function of the bZIP transcription factor HY5 in the UV-B response of *Arabidopsis*. *Proc Natl Acad Sci USA* **101**: 1397–1402
- Vanhaelewyn L, Prinsen E, Van Der Straeten D, Vandenbussche F** (2016) Hormone-controlled UV-B responses in plants. *J Exp Bot* **67**: 4469–4482
- Wang J, Ye B, Yin J, Yuan C, Zhou X, Li W, He M, Wang J, Chen W, Qin P, et al.** (2015) Characterization and fine mapping of a light-dependent leaf lesion mimic mutant 1 in rice. *Plant Physiol Biochem* **97**: 44–51
- Wang L, Pei Z, Tian Y, He C** (2005) OsLSD1, a rice zinc finger protein, regulates programmed cell death and callus differentiation. *Mol Plant Microbe Interact* **18**: 375–384
- Yamanouchi U, Yano M, Lin H, Ashikari M, Yamada K** (2002) A rice spotted leaf gene, *Spl7*, encodes a heat stress transcription factor protein. *Proc Natl Acad Sci USA* **99**: 7530–7535
- Yang Y, Liang T, Zhang L, Shao K, Gu X, Shang R, Shi N, Li X, Zhang P, Liu H** (2018) UVR8 interacts with WRKY36 to regulate HY5 transcription and hypocotyl elongation in *Arabidopsis*. *Nat Plants* **4**: 98–107
- Yang Y, Zhang L, Chen P, Liang T, Li X, Liu H** (2020) UV-B photoreceptor UVR8 interacts with MYB73/MYB77 to regulate auxin responses and lateral root development. *EMBO J* **39**: e101928
- Yi J, Lee YS, Lee DY, Cho MH, Jeon JS, An G** (2016) OsMPK6 plays a critical role in cell differentiation during early embryogenesis in *Oryza sativa*. *J Exp Bot* **67**: 2425–2437
- Yin K, Han X, Xu Z, Xue H** (2009) Arabidopsis GLP4 is localized to the Golgi and binds auxin in vitro. *Acta Biochim Biophys Sin* **41**: 478–487
- Yoshida S, Forno DA, Cock JH, Gomez KA** (1976) Laboratory manual for physiological studies of rice. International Rice Research Institute, Manila, Philippines.
- Zhang Y, Su J, Duan S, Ao Y, Dai J, Liu J, Wang P, Li Y, Liu B, Feng D, et al.** (2011) A highly efficient rice green tissue protoplast system for transient gene expression and studying light/chloroplast-related processes. *Plant Methods* **7**: 30–43
- Zhao J, Liu P, Li C, Wang Y, Guo L, Jiang G, Zhai W** (2017) *LMM5.1* and *LMM5.4*, two eukaryotic translation elongation factor 1A-like gene family members, negatively affect cell death and disease resistance in rice. *J Genet Genomics* **44**: 107–118
- Zhao SQ, Xiang JJ, Xue HW** (2013) Studies on the rice LEAF INCLINATION1 (LC1), an IAA-amido synthetase, reveal the effects of auxin in leaf inclination control. *Mol Plant* **6**: 174–187